PAPER

NJC
www.rsc.org/njc

Symmetry of van der Waals molecular shape and melting points of organic compounds

Yuri L. Slovokhotov,*[ab] Ivan S. Neretin[b] and Judith A. K. Howard[a]

[a] *Department of Chemistry, University of Durham, South Road, Durham, UK DH1 3LE E-mail: j.a.k.howard@durham.ac.uk; Fax: +44 (0191) 384 4737*
[b] *Institute of Organoelement Compounds, Russian Academy of Sciences, 28 Vavilov St., Moscow, Russia. E-mail: slov@ineos.ac.ru; Fax: +7 (095) 135 5085*

***Received* (in Durham, UK) 4th September 2003, Accepted 27th April 2004**
First published as an Advance Article on the web 28th June 2004

Long-known empirical regularities in melting points (mp) among molecular crystals of organic compounds with a closely related stoichiometry are dictated by a short-range molecular van der Waals term in their crystal field. This term, which acts as a symmetry-breaking perturbation on the averaged intermolecular interactions, is determined by the "contact" potential in the vicinity of molecules, *i.e.* by the shape of their van der Waals surface. To reflect the topology of the crystal field, an approximate *van der Waals group* $\check{G}$ of the average local field acting on a molecule and *asymmetry* a_s of the molecular surface composed of atomic van der Waals spheres, as its total misfit to $\check{G}$, were introduced. The scheme was applied to organic compounds whose molecules have a mirror symmetry plane; the shape of two-dimensional sections of their van der Waals surfaces by this plane was analysed. Calculated values of molecular asymmetry parallel as yet uninterpreted trends in melting point data such as oscillations between "even" and "odd" n-alkanes C_nH_{2n+2}, reduced melting temperatures of monosubstituted derivatives with highly-symmetric molecular cores (*e.g.* toluene), and non-trivial mp orders among the isomers of disubstituted ethylenes $C_2H_2X_2$ ("*gem-* < *cis-* < *trans-*"), substituted benzenes $C_6H_4X_2$ ("*meta-* < *ortho-* < *para-*"), $C_6H_3X_3$ ("1,2,4- < 1,2,3- < 1,3,5-"), $C_6H_2X_4$ ("1,2,3,5- < 1,2,3,4- < 1,2,4,5-"), and disubstituted naphthalenes. The observed mp trends do not display any notable correlation with molecular moments of mass and charge distribution, thus being dictated mostly by van der Waals forces.

Introduction

Diffraction studies of new compounds during the last 50 years have revealed atomic positions in more than 300 000 crystal structures which are now available from the Cambridge Structural Database (CSD)[1] and Inorganic Crystal Structure Database (ICSD).[2] Such a great number of well-characterised substances, usually with some reported bulk properties (colour, density, melting and/or boiling points, *etc.*) represents only the peak of a much larger number of all known organic and inorganic compounds, which presently includes more than 8 million "organic" entries and 1.9 million "inorganic" ones in Beilstein[3] and Gmelin[4] computer databases, respectively. However, this overwhelming experimental material is still only marginally explored by physicists, whose main research interests remain restricted to several hundreds of well known substances, often (though not always) of the simplest stoichiometry—like noble gases, small molecules, pure elements, and binary compounds. The expanding volume of physical data that continuously emerges as a by-product of chemical research has created a diverse field of physical chemistry, including crystallography of inorganic and organic compounds, structural chemistry, solid state chemistry, studies of molecules and interfaces, and many others. The structure of molecular crystals and other condensed phases of organic compounds, and their structure–property relationships, has become a subject of many excellent review books (see refs 5–9 and references therein). Recently, the whole content of "classical" physical chemistry has been slowly moving towards a new emerging physics of complex systems.[10]

Melting points and boiling points, being the most important physical constants of any substance for chemists during the last 200 years, have been measured for more than 1 million compounds. A relationship of these data to the atomic structure of molecules was extensively studied in the first half of the 20th century, when many non-trivial trends and regularities were established empirically.[11] Almost completely abandoned in the second half of the century due to the fast development of direct structural studies, this field is now reviving as a part of a renaissance in analysis of fundamental physical concepts. Recent studies on this topic use modern physical methods of characterisation, including single crystal X-ray diffraction as the most powerful tool.[12–14]

In this paper, we discuss melting points (mp) in different sets of organic compounds whose molecular structures were firmly established by physical methods. Starting from long-known correlations of mp with molecular geometry in these sets, we suggest a new concept of *van der Waals symmetry* as an approximate symmetry of a molecular surface built of atomic van der Waals spheres, that determines a structure-dependent attractive term in a molecular field. Deviations of a molecular surface from a given van der Waals point group (*i.e. molecular asymmetry*) may be calculated and compared in a set of related substances, showing a good correlation with mp (and possibly with other bulk properties related to a local molecular environment in a crystal). Application of van der Waals symmetry gives a physical basis to a search for structure–property correlations in the whole class of molecular crystals.

Melting points of organic compounds: selected data

Molecular crystals (*e.g.* of organic compounds) exist mostly due to van der Waals attractive forces between their molecules.[5–8] In the absence of strong electrostatic and specific intermolecular interactions, melting points of molecular

DOI: 10.1039/b310787f

Table 1 Melting points (T_m) and boiling points (T_b) in lower acyclic hydrocarbons[3]

Compound	Content	Formula	Point group[a]	T_m/K	T_b/K
C_3 family					
Propane	C_3H_8	$CH_3CH_2CH_3$	C_{2v}	83	231
Propene	C_3H_6	$CH_2{=}CHCH_3$	C_s	88	226
Propyne	C_3H_4	$HC{\equiv}CCH_3$	C_{3v}	171	250
Allene	C_3H_4	$CH_2{=}C{=}CH_2$	D_{2d}	137	238
C_4 family					
n-Butane	C_4H_{10}	$CH_3CH_2CH_2CH_3$	C_{2h}	135	272
Isobutane	C_4H_{10}	$(CH_3)_3CH$	C_{3v}	113	261
But-1-ene	C_4H_8	$CH_2{=}CHCH_2CH_3$	C_1	88	267
cis-But-2-ene	C_4H_8	$CH_3CH{=}CHCH_3$	C_2	134	277
trans-But-2-ene	C_4H_8	$CH_3CH{=}CHCH_3$	C_{2h}	167	273
2-Methylpropene	C_4H_8	$CH_2{=}C(CH_3)_2$	C_{2v}	133	266
Methylallene	C_4H_6	$CH_3CH{=}C{=}CH_2$	C_s	137	284
trans-Butadiene	C_4H_6	$CH_2{=}CHCH{=}CH_2$	C_{2h}	164	269
But-1-yne	C_4H_6	$CH{\equiv}CCH_2CH_3$	C_s	147	281
But-2-yne	C_4H_6	$CH_3C{\equiv}CCH_3$	D_{3h}	241	300
Buta-1,3-diyne	C_4H_2	$CH{\equiv}CC{\equiv}CH$	$D_{\infty h}$	237	283
C_5 family					
n-Pentane	C_5H_{12}	$CH_3CH_2CH_2CH_2CH_3$	C_{2v}	143	309
Isopentane	C_5H_{12}	$(CH_3)_2CHCH_2CH_3$	C_1	113	302
Neopentane	C_5H_{12}	$C(CH_3)_4$	T_d	256	283
Pent-1-ene	C_5H_{10}	$CH_2{=}CHCH_2CH_2CH_3$	C_1	108	303
cis-Pent-2-ene	C_5H_{10}	$CH_3CH{=}CHCH_2CH_3$	C_1	122	310
trans-Pent-2-ene	C_5H_{10}	$CH_3CH{=}CHCH_2CH_3$	C_1	137	309
2-Methyl-but-1-ene	C_5H_{10}	$CH_2{=}C(CH_3)CH_2CH_3$	C_1	136	304
2-Methyl-but-2-ene	C_5H_{10}	$CH_3C(CH_3){=}CHCH_3$	C_s	140	312
3-Methyl-but-1-ene	C_5H_{10}	$CH_2{=}CHCH(CH_3)_2$	C_1	105	293
Penta-1,4-diene	C_5H_8	$CH_2{=}CHCH_2CH{=}CH_2$	C_2	125	299
Penta-1,3-diene	C_5H_8	$CH_2{=}CHCH{=}CHCH_3$	C_s	186	315
Ethylallene	C_5H_8	$CH_3CH_2CH{=}C{=}CH_2$	C_1	136	318
1,3-Dimethylallene	C_5H_8	$CH_3CH{=}C{=}CHCH_3$	C_2	147	321
Pent-1-yne	C_5H_8	$CH{\equiv}CCH_2CH_2CH_3$	C_s	167	313
Pent-2-yne	C_5H_8	$CH_3C{\equiv}CCH_2CH_3$	C_s	164	329
Penta-1,4-diyne	C_5H_4	$CH{\equiv}CCH_2C{\equiv}CH$	C_{2v}	253	337
Penta-1,3-diyne	C_5H_4	$CH{\equiv}CC{\equiv}CCH_3$	C_{3v}	242 (233)[b]	350

[a] Highest possible molecular symmetry in appropriate conformation. [b] Inconsistent data.

crystals generally increase with the increase of molecular masses M, but strongly depend on molecular geometry where the molecules are big enough (*ca.* $\geq$10 atoms). Variations of mp among organic substances of close stoichiometry (*e.g.* isomers) are commonly believed to be due to different packing efficiency of their molecules[5–9]—a viewpoint that usually terminates further studies of their relationship because a quantitative packing analysis presents an unsolved problem of huge complexity. In this chapter, some empirically established linkages between mp and molecular structure are discussed briefly (see ref 11 for more information and references). Sources of experimental data are discussed below in more detail (see Calculations).

Acyclic hydrocarbons

A typical dependence of mp on molecular geometry is displayed by the lowest acyclic saturated and unsaturated hydrocarbons C_nH_m (Table 1). Melting points of these closely related compounds, whose molecular masses M are roughly constant within each C_n family, display variations up to 150 K (*e.g.* three isomers of pentane C_5H_{12}). In each family, those hydrocarbons with highest mp usually have highest molecular symmetry *and* rigid shape—*i.e.* a smaller number of possible symmetry-breaking conformational changes (like neopentane CMe_4 in comparison with *n*-pentane $CH_3(CH_2)_3CH_3$, where Me = CH_3). Distortions of all-*trans* linear carbon chain by side fragments (branches) and isolated double bonds that tend to undergo eclipsed orientation relative to the neighbouring C–H bond (Scheme 1), diminish molecular symmetry and lead to lower mp values. Boiling points in the same families vary in narrower ranges, but show a generally similar trend with larger fluctuations and some outlier data (*e.g.* neopentane CMe_4 which has the highest melting point and the lowest boiling point in the whole C_5 family) due to less local order in liquids than in crystals.† Similar trends persist in the mp's of heavier acyclic hydrocarbons; representative examples of C_6–C_8 families are displayed in Table 2. High-melting substances are composed of rigid ribbon-like (conjugated linear all-*trans*-polyenes), rod-like (conjugated polyynes) and spheroid molecules. It is noteworthy that the crystalline linear alkanes

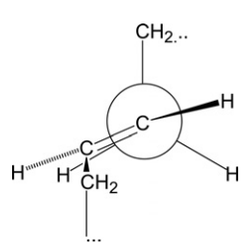

Scheme 1 A preferred conformation of –CH_2–CH=CH– fragment in linear alkenes breaking the planar all-*trans* geometry of a carbon chain (CSD).

† Boiling points in substituted hydrocarbons were analysed elsewhere.[15]

Table 2 Melting points *vs.* molecular symmetry in higher acyclic hydrocarbons

Compounds	Highest molecular symmetry	T_m/K
C_6 family		
Branched hexanes, *n*-hexenes, non-conjugated dienes	C_1, C_s, C_i	120–150
Me_3CCH_2Me	C_s	173
n-C_6H_{14}	C_{2h}	178
$MeC{\equiv}CCH_2CH_2Me$, $EtC{\equiv}CEt$, $MeCH{=}CHCH{=}CHMe$	C_s, C_2, C_{2h}	150–175
$Me_2C{=}CMe_2$	D_{2h}	199
$HC{\equiv}CC{\equiv}CC{\equiv}CH$	$D_{\infty h}$	253
trans-$CH_2{=}CHCH{=}CHCH{=}CH_2$	C_{2h}	261
$HC{\equiv}CCH_2CH_2C{\equiv}CH$	C_{2h}	268
$MeC{\equiv}CC{\equiv}CMe$	D_{3h}	338
C_7 family		
Branched heptanes, *n*-heptenes, hepta-1,6-diene	C_1, C_s	130–165
n-C_7H_{16}	C_{2v}	182
$Me_3CC{\equiv}CMe$	C_{3v}	191
$HC{\equiv}C(CH_2)_4CH_3$, $Me_3CCH_2C{\equiv}CH$, $HC{\equiv}C(CH_2)_3C{\equiv}CH$,	C_s, C_2	185–200
Me_3CCHMe_2	C_s	249
$MeC{\equiv}CC{\equiv}CC{\equiv}CH$	C_{3v}	290
trans-$MeCH{=}CHCH{=}CHCH{=}CH_2$	C_s	295
C_8 family		
Branched octanes, *n*-octenes	C_1, C_2, C_s	140–185
$HC{\equiv}C(CH_2)_5CH_3$	C_s	194
$MeC{\equiv}C(CH_2)_4Me$	C_s	211
n-C_8H_{18}	C_{2h}	216
$HC{\equiv}C(CH_2)_4C{\equiv}CH$	C_{2h}	241
$MeC{\equiv}C(CH_2)_2C{\equiv}CMe$	C_{2h}	300
trans-$CH_2{=}CHCH{=}CHCH{=}CHCH{=}CH_2$	C_{2h}	323
Me_3CCMe_3	D_{3d}	374
$MeC{\equiv}CC{\equiv}CC{\equiv}CMe$	D_{3h}	402

C_nH_{2n+2} that have planar zigzag all-*trans* conformation show regular "even–odd" modulations of mp up to $n = 26$–30.[11] Recent single crystal X-ray studies,[12,13] in excellent agreement with the results obtained in the mid-20th century,[5,11] revealed regular differences in packing of chain hydrocarbon derivatives with even and odd numbers of carbon atoms—which is an important fact, but hardly the most fundamental reason for the effect.

It should be noted that a correlation between mp and the ideal molecular symmetry of hydrocarbons is not particularly strict, and examples of both high-melting substances with low exact point symmetry (*e.g.* *trans*-heptatriene $MeCH{=}CHCH{=}CHCH{=}CH_2$) and medium- and low-melting phases with rather high molecular symmetry (isobutane $CHMe_3$, tetramethylethylene $Me_2C{=}CMe_2$), are known. Also noteworthy is the fact that mp data[3] presented in Table 1 are not available for all known hydrocarbons even in the C_5 family whereas a substantial part of all C_9, C_{10} and higher hydrocarbons possible on geometric and chemical grounds have never been synthesised. Data in Tables 1 and 2 point to molecular origins of mp variations—so some direct link between geometry of molecules and their packing efficiency has to be revealed.

Reduction of mp by broken molecular symmetry

Although the mp of a molecular crystal is not always determined by the point group of its molecules, it is strongly influenced by symmetry in some well-established cases. Thus, organic and organometallic substances composed of highly-symmetric molecules like benzene C_6H_6, cyclohexane C_6H_{12}, ferrocene $(C_5H_5)_2Fe$, carboranes $C_2B_{10}H_{12}$ *etc.* usually have higher mp's than their derivatives with higher molecular mass, whose symmetry is reduced by attached side fragments (Table 3), in particular when these fragments do not participate in specific intermolecular binding as in nitrobenzene (mp 279 K) or phenol (mp 361 K). Fig. 1 presents a typical linear correlation of mp with molecular mass M in semi-logarithmic coordinates for hexasubstituted benzenes C_6X_6 together with substantially reduced melting points of monosubstituted benzenes C_6H_5X and pentachlorobenzenes C_6Cl_5Y (where X,Y = H, Me or halogen). Although polyfluorinated species like hexafluorobenzene C_6F_6 generally have a lower mp due to unfavourable,[16] *i.e.* destabilising F···F intermolecular interactions, monofluorinated derivatives in Fig. 1 do not deviate significantly from the general trend. Boiling points in the same sets, where available, regularly increase with M.

Decrease ΔT of mp in benzene derivatives with broken molecular symmetry are roughly proportional to "steric perturbation", *i.e.* to an absolute difference in van der Waals volumes $\Delta V = V_X - V_H$ or $V_Y - V_{Cl}$ of X (Y) substituent and other vicinal atoms at C_6 hexagon (Fig. 2). A linear correlation in the ΔT *vs.* ΔV plot, in the C_6Cl_5Y series with negative ΔV for Y = H and F, points to rather small changes of the total van der Waals field of a substituted molecule (so justifying the word "perturbation"). A similar trend is observed in other compounds with a monosubstituted high-symmetry core, including *tert*-alkyl derivatives (*cf.* strong decrease of mp from CMe_4 to Me_3CCH_2Me and from C_2Me_6 to C_2Me_5H in Tables 1, 2). As in the case of acyclic hydrocarbons, the ideal molecular symmetry evidently matters less than total molecular shape. It is particularly evident for derivatives of *o*-, *m*- and *p*-carboranes $C_2B_{10}H_{12}$ whose strict molecular symmetry is low for the *o*- and *m*- and high for the *p*-isomer, whereas the molecular

Table 3 Melting points in some monosubstituted derivatives of high-symmetric molecules

Compound	Formula	M	Molecular symmetry	T_m/K
Benzene	C_6H_6	78	D_{6h}	279
Toluene	C_6H_5Me	92	C_{2v}	178
Iodobenzene	C_6H_5I	204	C_{2v}	242
Cyclohexane	C_6H_{12}	84	D_{3d}	280
Methylcyclohexane	$C_6H_{11}Me$	98	C_s	146
Bromocyclohexane	$C_6H_{11}Br$	163	C_s	216
Ferrocene	$(C_5H_5)_2Fe$	186	D_{5d}	447
Methylferrocene	$(C_5H_5)Fe(C_5H_4Me)$	200	C_s	310
Fluoroferrocene	$(C_5H_5)Fe(C_5H_4F)$	204	C_s	389
Chloroferrocene	$(C_5H_5)Fe(C_5H_4Cl)$	220	C_s	330
Bromoferrocene	$(C_5H_5)Fe(C_5H_4Br)$	265	C_s	304
Iodoferrocene	$(C_5H_5)Fe(C_5H_4I)$	312	C_s	318
o-Carborane-12	o-$C_2B_{10}H_{12}$	144	C_{2v}	568
m-Carborane-12	m-$C_2B_{10}H_{12}$	144	C_{2v}	545
p-Carborane-12	p-$C_2B_{10}H_{12}$	144	D_{5d}	533
9-Chloro-*o*-carborane-12	o-$C_2B_{10}H_{11}Cl$	179	C_1	494
9-Chloro-*m*-carborane-12	m-$C_2B_{10}H_{11}Cl$	179	C_1	505
9-Iodo-*o*-carborane-12	o-$C_2B_{10}H_{11}I$	270	C_1	397
9-Iodo-*m*-carborane-12	m-$C_2B_{10}H_{11}I$	270	C_1	382
Naphthalene	$C_{10}H_8$	128	D_{2h}	353
1-Methylnaphthalene	$C_{10}H_7Me$	140	C_s	242
2-Methylnaphthalene	$C_{10}H_7Me$	140	C_s	307
1-Iodonaphthalene	$C_{10}H_7I$	254	C_s	277
2-Iodonaphthalene	$C_{10}H_7I$	254	C_s	328

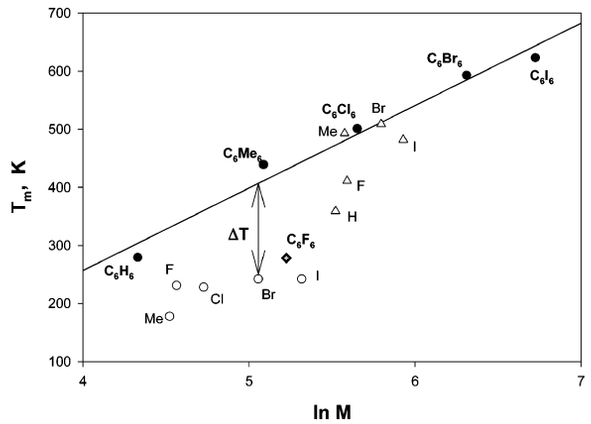

Fig. 1 A linear trend in mp increase with ln$M$ (where M is molecular mass in a.m.u.) in *sym*-hexasubstituted benzenes C_6X_6 (filled circles) and reduced mp in monosubstituted benzenes C_6H_5X (open circles) and perchlorobenzenes C_6Cl_5Y (open triangles). Substituents X and Y are shown at the corresponding points. Melting point decrease ΔT is denoted by double arrow. Hexafluorobenzene with strongly reduced melting point (diamond symbol) was excluded from the linear correlation.

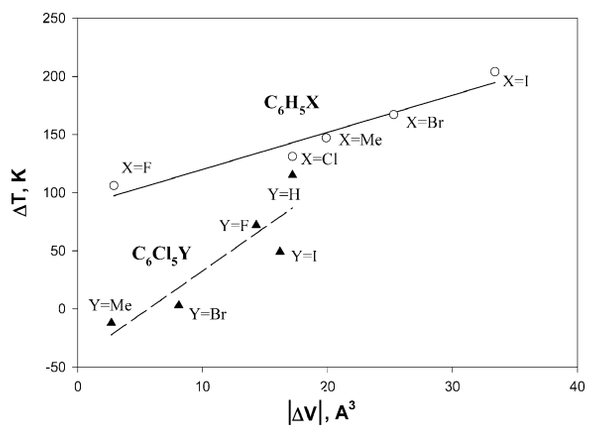

Fig. 2 Linear correlation between mp decrease ΔT (see Fig. 1) of monosubstituted benzenes C_6H_5X (open circles, solid line) and perchlorobenzenes C_6Cl_5Y (filled triangles, dashed line), with absolute differences of van der Waals volumes (taken from ref 18) of substituents $|\Delta V|$ (where ΔV is $V_X - V_H$ and $V_X - V_{Cl}$).

shape is very close in all three cases (see Table 3). Also noteworthy in Table 3 is a different reduction of mp in monosubstituted naphthalenes $C_{10}H_7X$ with the X fragment in the 1- and 2- positions (for numbering see Scheme 2). This experimental fact reveals a variable, geometry-dependent strength of $D_{2h} \rightarrow C_s$ symmetry breaking in two isomers that belong to the same point group.

Substituted benzenes and related substances

One of the best known, but as yet not interpreted, examples of structure–property relationships in organic chemistry, is regular "$m < o < p$" mp variations (where '<' corresponds

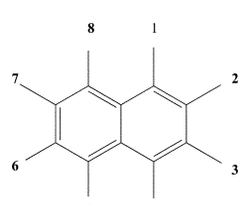

Scheme 2 Positions of substituents on the naphthalene moiety.

to increase of a temperature from left to right) in *ortho*- (*o*-), *meta* (*m*-) and *para*- (*p*-) isomers of disubstituted benzenes $C_6H_4X_2$ and C_6H_4XY (see refs 11,14). Melting points of the isomers may vary within 100–110 K for a broad range of (X,Y) substituents with very different steric and electronic characteristics. The observed "$m < o < p$" sequence looks mysterious, since most molecular parameters of the isomers like moments of mass and charge distributions increase or decrease uniformly in *o*–*m*–*p* order. A recent thorough study of this problem by Boese and co-workers in the case of $C_6H_4Cl_2$ isomers[14] actually showed that the effect can hardly be interpreted using even a rigorous analysis of molecular packing. One of the few exclusions from the general trend of the *para*-isomer having the highest mp is *p*-diethylbenzene which melts at 12 K lower than its *o*-isomer. A recent single crystal X-ray study of *o*- and *p*-$C_6H_4Et_2$ showed that the Et fragments are twisted out of the plane of the benzene ring in both molecules which may be a reason for the inverted mp order; parameters of their van der Waals shape are presently under calculation.[17] More systematic deviations from the "$m < o < p$" rule, shown in Table 4, have low-melting *ortho*-C_6H_4XY derivatives with bulky planar (or almost planar) X substituents (NO_2, C(O)X, NMe_2, *etc.*) twisted out of the plane of the benzene ring for steric reasons (CSD data).

It is interesting to note that H-bonded benzene derivatives that melt higher than pure van der Waals crystals of the same molecular masses also obey the "$o < m < p$" rule in most cases. However, some *o*-isomers in these compounds [*e.g.* catechol *o*-$C_6H_4(OH)_2$ mp 378 K] melt at lower temperatures than the *meta*-isomers [resorcinol *m*-$C_6H_4(OH)_2$, mp 384 K] due to formation of H-bonded dimers which diminishes the number of OH groups participating in a 3D network of hydrogen bonding. Boiling points of disubstituted benzenes without specific X···X interactions usually vary within 5–10°; however, they may be reduced by as much as 30–40° for *o*-isomers of H-bonded species (see Table 4). So the molecular structure of disubstituted benzenes looks responsible both for the "$m < o < p$" trend in mp *and* the most typical deviations from it. Difluorobenzenes and other polyfluorinated arenes have reduced melting points but generally obey the same order.

In Scheme 3, more general melting point regularities in substituted benzenes $C_6H_nX_{6-n}$ and disubstituted ethylenes $C_2H_2X_2$ that follow the "$m < o < p$" rule, are shown. Unlike

Table 4 Examples of disubstituted benzenes deviating from the "$m < o < p$" mp trend

	Melting points/K			Boiling points (760 torr)/K		
Compound	*o*-	*m*-	*p*-	*o*-	*m*-	*p*-
$C_6H_4Et_2$	242	189	230	456	454	457
$C_6H_4I_2$	300	310	403	559	558	558
$C_6H_4(CN)_2$	413	434	495	—	—	—
$C_6H_4(NC)_2$	356	377 (350)[a]	439	—	—	—
$C_6H_4(CN)NC$	—	—	448	—	—	—
$C_6H_4(Me)NO$	345	326	321	—	—	—
$C_6H_4(Cl)NO_2$	307	319	357	519	509	515
$C_6H_4(Br)NO_2$	316	329	400	531	538	529
$C_6H_4(OH)NO_2$	319	370	387	489	—	552
$C_6H_4(OH)Cl$	282	306	317	448	487	491
$C_6H_4(OH)Br$	279	306	339	468	509	511
$C_6H_4(Br)COOH$	423	428	527	—	—	—
$C_6H_4(I)COOH$	436	461	543	506	551	550
$C_6H_4(Me)COOH$	381	385	455	532	536	548
$C_6H_4(Br)CONH_2$	431	429	463	—	—	—
$C_6H_4(I)CONH_2$	456	458	488	—	—	—

[a] Inconsistent data.

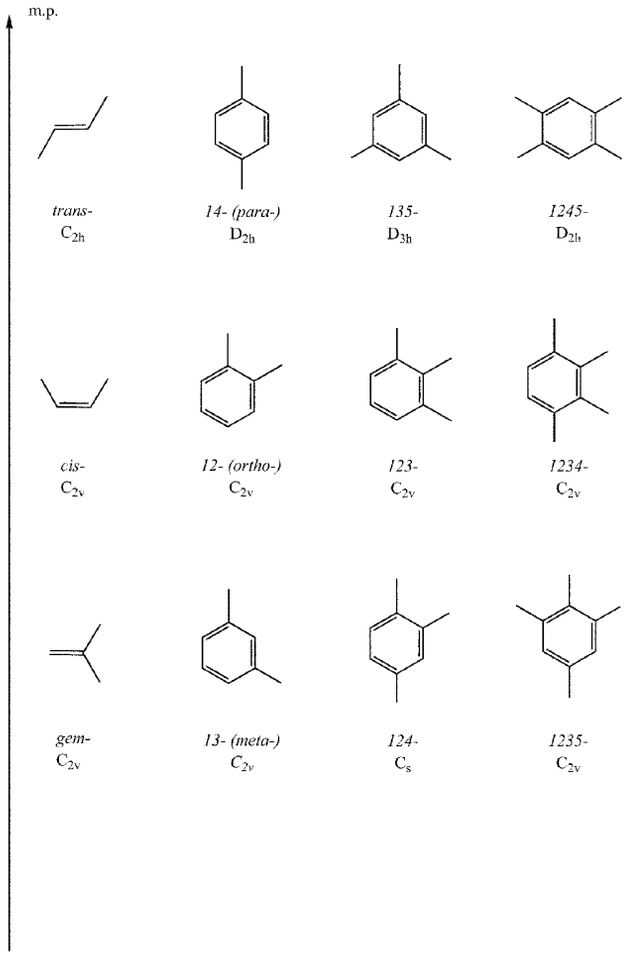

Scheme 3 A preferred order of melting points (mp) among isomers of disubstituted ethylenes $C_2H_2X_2$ and substituted benzenes $C_6H_{6-n}X_n$ ($n = 2$–4) from Beilstein data.[3] Notations of isomers and their ideal molecular point groups are shown.

small hydrocarbons, the planar carbon skeletons of the molecules in all these sets are conformationally rigid. In each set, the isomer of highest symmetry usually has the highest mp. Exceptions are disubstituted ethylenes where *gem*-, *cis*- and *trans*-isomers have point groups of the same order of 4. The low-melting isomer has the lowest symmetry only in trisubstituted arenes (1,2,4-$C_6H_3X_3$, C_s), since *m*- and *o*-isomers of $C_6H_4X_2$, as well as 1,2,3,5- and 1,2,3,4-isomers of $C_6H_2X_4$, that have, respectively, lowest and medium mp in their sets, belong to the same point group C_{2v}. As in disubstituted benzenes, some particular substances in other families may deviate from the general trend. Similarly, the substituents responsible for specific intermolecular interactions usually uniformly elevate (NO_2, OH, COOH) or uniformly lower (F) the mp's for all isomers, though they may also affect their order in some cases. In a few complete sets of *o*-, *m*-, and *p*-isomers studied at the same (or similar) temperatures that are available from the CSD, the high-melting isomer does not always have the highest relative density of packing, *i.e.* lowest unit cell volume per molecule V/Z (Table 5). Since variations in V/Z for different isomers are close to the errors in unit cell volume that may be as large as 2–3 Å^3, a packing analysis can hardly provide decisive arguments to a study of mp regularities.

Disubstituted naphthalenes and related substances

Variations in melting points of ten isomers of *sym*-disubstituted naphthalenes $C_{10}H_6X_2$ may be as high as 150 K (Table 6). As in substituted benzenes, the existence of four highest-melting (1,5-, 2,3- 2,6- and 2,7-) isomers with higher molecular symmetry (C_{2v} or C_{2h}), four lowest-melting "dissymmetric" ones (1,2-, 1,3-, 1,6-, and 1,7- with only one mirror plane, C_s symmetry) and two "intermediate" 1,4- (C_{2v}) and 1,8-isomers (C_2) with variable relative mp's in different sets, is observed for various X substituents. Six of the ten difluoronaphthalenes $C_{10}H_6F_2$ with available mp obey the same regularity. However, this trend may be modified in NO_2 and OH-substituted species. Melting points of the hetero-disubstituted $C_{10}H_6XY$ species (15 isomers) vary less regularly over a slightly more narrow range (<100 K). In heavier condensed arenes, mp data are not available for all $C_{14}H_8X_2$ disubstituted anthracenes (15 geometric isomers) and disubstituted phenanthrene (25 isomers). Fifteen known dimethylanthracenes show a similar trend to the dimethylnaphthalenes, with the addition of a new high-melting 9,10-isomer (D_{2h}), whereas 21 known dimethylphenanthrenes have less regular variations in mp, within a range of 160 K. Also noteworthy is the higher melting point of unsubstituted anthracene $C_{14}H_{10}$ (D_{2h}, 489 K) in comparison with the unsubstituted phenanthrene $C_{14}H_{10}$ (C_{2v}, 374 K) which agrees with the above regularities. These two condensed polyarenes have, respectively, three and five sets of monosubstituted isomers with different amounts of mp reduction. Empirical mp trends in polysubstituted naphthalenes and substituted diphenyls, as well as in some other aromatic compounds (*e.g.* pyrenes) are not analysed here because of space limits.

A notable trend for disubstituted naphthalenes, which parallels substituted benzenes, is the lowering of the mp for 2,3-isomers with planar (or almost planar) bulky fragments twisted out of the molecular plane, as well as for other species with two bulky substituents in the 1,8-positions, which distort the planar geometry of the C_{10} naphthalene core for steric reasons (CSD). As in disubstituted benzenes, two neighbouring OH groups significantly reduce the mp in the corresponding isomers in comparison with other dihydroxo-naphthalenes—most probably due to formation of H-bonded pairs that inhibit these groups from participating in a three-dimensional intermolecular H-bonding network. Such H-bonded dimers were actually observed in the crystal structure of 2,3-$C_{10}H_6(OH)_2$ (see Table 6 for reference).

Symmetry of the molecular van der Waals surface

Most organic compounds display a high degree of similarity in characteristics such as crystal lattice energy (5–10 kJ mol^{-1} per C atom), Kitajgorodsky's packing coefficient (0.65–0.80) and molecular coordination number (12).[5,8,18] This similarity allows for a simple additive representation of molecular crystals as dense packing of rigid three-dimensional molecular "bodies" terminated by their van der Waals surfaces.[5] However, the melting points of molecular crystals are evidently determined by their total intermolecular potential which cannot be represented quantitatively by such a simple scheme. Nevertheless, a drastic simplification of theory is still possible if the observed mp trends may be linked to some specific term in a total van der Waals crystal field U which does obey additivity.

A strong correlation of mp with molecular geometry of organic compounds points indeed to a virtual short-range ("contact") character of the influence of van der Waals forces on the bulk properties of crystals composed of medium-size molecules. Although the van der Waals attractive term ($\sim r^{-6}$, where r is intermolecular distance) may have a measurable effect up to 10–100 nm[8], about 90% of the whole energy of intermolecular interactions for a given molecule within a bulk phase derives from its environment inside a sphere of a radius $R \leq 1$ nm[18] where a molecular structure should be taken into account. Due to the large number of neighbouring atoms of a bulk phase in such a sphere, the field created by any

Table 5 Packing characteristics and melting points (T_m) of C_6H_4XY isomers stored in CSD (*p*-di-isonitrilobenzene shown for comparison)

Compound	*M*	Temp. of an X-ray study/K	(V/Z)/Å^3	d_{calc}/g cm^{-3}	T_m/K	CDS refcode
$C_6H_4Cl_2$ o-	147	223	159.0	1.535	256	ABUMIT
m-		220	160.9	1.518	298	ABUMOZ
p-		260	153.6	1.590	326	DCLBEN04
$C_6H_4(NO_2)_2$ *o*-	168	295	177.5	1.573	392	ZZZFYW01
m-			177.8	1.569	363	DNBENZ01
p-			172.5	1.618	447	DNITBZ11
$C_6H_4(CN)_2$ o-	128	295	170.4	1.249	413	YUYPUD
m-			165.8	1.284	434	OBIZEE
p-			165.6	1.285	495	TEPNIT05
$C_6H_4(NC)_2$ *p*-	128	295	168.8	1.260	439	ZZZIZA01
$C_6H_4(OH)_2$ *o*-	110	295	135.7	1.347	378	CATCOL
m-			136.7	1.337	384	RESORA02
p-			134.0	1.364	447	HYQUIN
o-$C_6H_4(NH_3^+)(COO^-)$	137	295	161.6	1.409	418	AMBACO01
m-$C_6H_4(NH_2)(COOH)$			165.3	1.378	448	AMBNZA
p-$C_6H_4(NH_2)(COOH)$			166.5	1.367	461	AMBNAC01
$C_6H_4(Cl)(CONH_2)$ *o*-	155	295	190.6	1.356	414	CLBZAM10
m-			186.0	1.389	407	NABRAJ
p-			179.4	1.444	451	PCBZAM01
$C_6H_4(Me)OH$ *o*-	108	223	154.3	1.164	304	OCRSOL
m-		173	159.4	1.127	285	MCRSOL
p-[a]		295	149.3	1.102	306	CRESOL02
p-[a]		295	162.9	1.202	310	CRESOL10

[a] Two polymorphs.

particular molecule in its "distant" part is randomised by interference and mutual screening. A reason for mp *vs.* structure correlations must therefore lie in the close contact region around the molecule where the molecule's field is not biased by the environment. The fact that most of the substances that display such correlations differ in their molecular packing (CSD; see also ref 14) confirms a fast decay of the structurally sensitive van der Waals term with increase of distance.

A local non-valence field in the immediate vicinity of molecules is qualitatively represented in chemistry by a shape of molecular surface built of van der Waals spheres of its atoms—*i.e.* by space-filling models. Dimensions of this surface are determined by molecular geometry and van der Waals radii that accumulate numerous data from structural and other physical studies.[5,18,19] A number of molecular shape parameters like volume, surface, sphericity, self-packing coefficient *etc.*[18] were invented to tackle particular problems in molecular crystals, but they are generally of less help when a broader range of data is considered.

Point symmetry is a local molecular characteristic that influences many bulk properties and shows some relationship with the mp's (see above). However, classical molecular structure represented by positions of atomic nuclei, as well as point group, are not completely relevant to molecular van der Waals interactions, because they ignore the fundamental property of a molecule to occupy a definite volume in the bulk phase.[5] Instead, we will analyse a symmetry of space-filling molecular models mentioned in the previous paragraph. A continuous

Table 6 Melting points T_m in *sym*-disubstituted naphthalenes $C_{10}H_6X_2$ (10 isomers) from the Beilstein database[3] and their packing characteristics available from CSD. For $C_{10}H_6Br_2$, calculated asymmetries a_s of molecular van der Waals sections in the D_{2h} group are shown in italics (see Results and discussion)

	Melting point (T_m/K) *vs.* molecular volume[a] (V/Z)/Å^3											
	X = Me		X = Cl		X = Br			X = NO_2		X = OH		X = F	
Isomer	T_m	V/Z	T_m	V/Z	T_m	V/Z	a_s[aa]	T_m	V/Z	T_m	V/Z	T_m	V/Z
1,2-	271		308	216.3[f]	341		0.073	434	237.0[o]	377		—[bb]	
1,3-	268		334	218.8[g]	336		0.110	418		397		–	
1,4-	280		339	214.3[h]	356	228.1[k]	0.067	404	229.3[p]	463	196.9[t]	305	
1,5-	354	226.3[b]	379	218.0[i]	404	221.8[l]	0.043	490		533	188.4[u]	342	187.9[y]
1,6-	258		321		331		0.096	438		409		–	
1,7-	259		335		347		0.094	429	229.4[q]	451	195.9[v]	—	
1,8-	337	229.4[c]	362		381	231.4[m]	0.052 + *x*[cc]	444	243.0[r]	415		313	187.7[z]
2,3-	377	231.3[d]	393		413		0.051	447	223.5[s]	433	194.1[w]	334	
2,6-	383	231.1[e]	409	216.7[j]	432	227.9[n]	0.035	552	237.0◦	490	199.4[x]	345	
2,7-	369		388		413		0.063	507		463		335	

[a] Single crystal X-ray diffraction data at room temperature (refcodes below): [b] DIMNAP01, [c] DMNAPH [d] DILKEO, [e] DMNPTL01, [g] ZZZJNW, [g] ZZZNHW, [h] DCLNAQ, [i] CLNAPH, [j] DCNAPH01, [k] DBRNAQ01, [l] COXLOQ, [m] COXLUW, [n] DBRNAP, [o] TEBHAJ, [q] DNNAPH, [q] DNTNAP01, [r] SAHSID, [s] ZZZMEG, [t] NPHHQU10, [u] VOGRUE, [v] NPHDLD, [w] VOGSEP, [x] VOGSAL, [y] DFNAPH10, [z] FLNAPH [aa] Molecular asymmetry in van der Waals group D_{2h} (see text). [bb] Not available. [cc] Should be corrected to non-planarity of naphthalene core.

character of these models requires a continuous description of their symmetry using the deviation of the molecular van der Waals surface from a given point group.

Based on the similarity of overall molecular packing patterns mentioned above, one may split the total van der Waals crystal field into two components:

$$U = U_0 + W \quad (1)$$

where U_0 is the average crystal field and W is a local contact term responsible for mp trends. The U_0 term, as a sum of the field from all molecules at all distances, has a high symmetry due to randomisation (see above). The topology of the W term is represented by the molecular van der Waals surface composed of atomic spheres. Differences in the W term between closely related molecules (*e.g.* isomers), in the first approximation, are proportional to a misfit in their van der Waals volumes.[5,18]

Local and structure-sensitive perturbations W of the crystal field U_0 may be analysed using group theory formalism. We call *molecular van der Waals group* a point group $\check{G}$ whose elements approximate a symmetry of the molecule's van der Waals surface, built of van der Waals spheres of its atoms. Symmetry operators $\{\check{g}_i\}$ of this group are placed in space to minimise a misfit between the 3D body of the molecule and its image transformed by $\check{g}_i$. Such a misfit is quantitatively represented by a continuous parameter: *molecular asymmetry* a_s:

$$a_s(\check{g}_i) = \Delta V / V_0 \quad (2)$$

for operation $\check{g}_i$, and

$$a_s(\check{G}) = (1/N)\sum a_s(\check{g}_i) \quad (3)$$

averaged over group $\check{G}$, where ΔV is a total volume of non-overlapping parts of the molecule, V_0 is total molecular volume, N is number of operations in $\check{G}$ (group order), and summation is taken over all elements $\check{g}_i \in \check{G}$. Asymmetry $a_s(\check{G})$ quantifies deviations of a molecule from a symmetry $\check{G}$; $a_s(G) = 0$ when the symmetry G is exact. If a group $\check{G}$ coincides with a symmetry of the average U_0 term in the crystal field, a strength of perturbation W is proportional to a misfit of the molecule to U_0, *i.e.* to the asymmetry $a_s(\check{G})$:

$$W \sim \Delta V \sim a_s(\check{G}), \quad (4)$$

where ΔV stands, as above, for deviations of molecular van der Waals volume from $\check{G}$. Asymmetry of a molecular shape, as a continuous parameter of its fitness to a given point group, is better in analysis of continuous experimental data (*e.g.* melting points) than discrete, exact symmetry of a molecular structure.

On a very qualitative level, molecules of two isomers **1** and **2** that belong, respectively, to point groups $G_1, G_2 \subset \check{G}$ will create the corresponding perturbations W_1 and W_2 of the average crystal field U_0. This field is roughly the same for both isomers because of the same atomic content of their molecules and a randomisation with increase in distances. Steric perturbations will deform a potential surface U_0 around each molecule in the crystal with a strength proportional to the molecular asymmetries $a_s^{(i)}(\check{G})$ ($i = 1,2$). If, for simplicity, the group $\check{G}$ corresponds to a very high symmetry (*e.g.* face centred cubic arrangement) where all closest neighbouring positions are subdivided by a barrier of the same height ΔU_0, and a crystal may be considered in the framework of classical mechanics, the perturbations W_i will cause a splitting of this barrier into a continuous energy interval from ΔU_{min} to ΔU_{max} (Fig. 3a,b). (In a quantum case, which is more familiar to chemists, a discrete degenerate energy level may split into several discrete sublevels by a reduction of molecular symmetry). Due to splitting, the potential barrier will be lowered in some directions around a molecule in the crystal, which allows the molecules to leave their positions with less kinetic energy—*i.e.* reduces the melting point of a substance. The amount of such reduction will be proportional to a strength of perturbation W_i, *i.e.* to the molecular asymmetry $a_s^{(i)}(\check{G})$; the isomers with higher asymmetry will have the lower melting points (Fig. 3c).

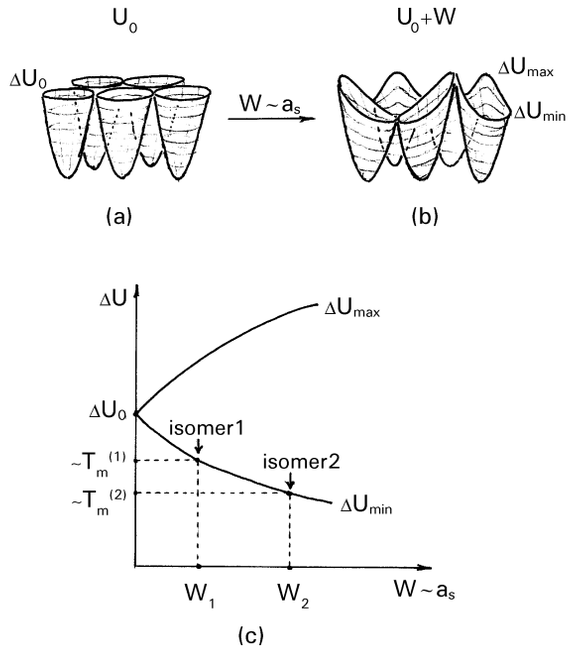

Fig. 3 (a,b) Deformation of van der Waals potential barriers between neighbouring energy minima that correspond to molecular positions in a crystal, by a symmetry-lowering steric perturbation W (schematically); (c) continuous smearing of the potential barrier ΔU_0 into energy interval by the perturbation for hypothetical isomers **1** (W_1) and **2** ($W_2 > W_1$). A stronger perturbation causes stronger splitting that lowers ΔU_{min} and brings a stronger reduction in the corresponding melting point $T_m^{(i)}$ for the isomer **2**: $T_m^{(2)} < T_m^{(1)}$.

In this paper, we use ~ (tilde) above the symbol and grey half-tone lines in the figures for approximate groups and their symmetry operations. Evidently, many approximate van der Waals groups may be applied to the same molecule. To define the "better" approximation, a weighted group order is used:

$$\Delta = N\exp(-\gamma a_s) \quad (5)$$

where γ is an empirical scale that allows us to distinguish between an exact group G_1 of order N_1 (for which $a_s^{(1)} = 0$) and approximate group $\check{G}_2$ of a higher order $N_2 > N_1$ with non-zero asymmetry $a_s^{(2)} > 0$:

$$\Delta_2 = N_2\exp(-\gamma a_s^{(2)}) < N_1, \ i.e.$$
$$\ln N_2 - \gamma a_s^{(2)} < \ln N_1, \ \text{so}$$
$$\gamma > (1/a_s^{(2)})\ln(N_2/N_1)$$

Calculations

Approximate van der Waals groups for organic molecules and their molecular asymmetries a_s were calculated by an original program for *n*-alkanes, disubstituted ethylenes, substituted arenes, and disubstituted naphthalenes. In the present study, we considered only molecules with an exact mirror plane σ_h whose point groups $\check{G}$ are direct product $\check{G}' \times C_s$. Therefore, $\check{G}'$ groups were applied to sections of van der Waals molecular surface (*e.g.* C_{2v} group of a section corresponds to D_{2h} group of a molecule), and formula (2) becomes

$$a_s(\check{g}_i) = \Delta S / S_0 \quad (2a)$$

where ΔS is the total misfit area when a section is transformed by element $\check{g}_i \in \check{G}'$, and S_0 is the total area of the original section.

Table 7 Molecular masses (M), asymmetries of van der Waals sections in C_{2v} group (a_s), experimental ($T_m^{exp.}$) and calculated ($T_m^{calc.}$) melting points for n-alkanes C_nH_{2n+2}

Compound	M	a_s	$T_m^{exp.}$/K	$T_m^{calc.}$/K
C_3H_8	44	0.0542	83	84
C_4H_{10}	58	0.0433	135	137
C_5H_{12}	72	0.0504	143	146
C_6H_{14}	86	0.0431	178	181
C_7H_{16}	100	0.0478	182	188
C_8H_{18}	114	0.0428	216	213
C_9H_{20}	128	0.0460	222	219
$C_{10}H_{22}$	142	0.0412	243	240
$C_{11}H_{24}$	156	0.0421	247	249
$C_{12}H_{26}$	170	0.0395	263	264
$C_{13}H_{28}$	184	0.0406	267	270
$C_{14}H_{30}$	198	0.0389	279	282
$C_{15}H_{32}$	212	0.0393	283	289

The $a_s(\check{g}_i)$ values defined this way were then used to calculate the total asymmetry $a_s(\check{G})$ by means of formula (3).

Approximate vertical symmetry planes σ_v and other elements applied to a molecular section were chosen by the following algorithm:

(1) All exact symmetry elements of the molecular section were retained.

(2) All new approximate symmetry elements passed through the geometric centre of section.

(3) The position of the first new symmetry plane σ_v (*e.g.* for C_2 or C_1 exact symmetry of section) was chosen to cut the section into halves of the equal $S_0/2$ areas.

(4) When under these conditions a choice of σ_v remained arbitrary, its position was fitted to minimise ΔS and so $a_s(\sigma_v)$.

(5) Next approximate elements $\{\check{g}_i\}$ were added to the first plane σ_v and/or to existing exact symmetry elements according to general rules for point groups.[20]

Molecular geometry of substituted ethylenes, arenes and naphthalenes was optimised by quantum chemistry calculations (GAUSSIAN 98[21] at semiempirical PM 3 level). The optimised geometry usually agreed with the experimental one within 0.01–0.02 Å in bond lengths and 2–3° in bond angles. For n-alkanes, idealised geometry was used (bond lengths C–C 1.54 Å, C–H 1.09 Å, bond angles CCC and CCH 109.5°). Atomic van der Waals radii were taken from Bondi.[19] Calculated asymmetries of molecular sections are presented in Tables 6–8 and Figs. 4, 6 and 8.

Melting and boiling points were extracted from Beilstein[3] and Gmelin[4] databases. Data from several authors for the same substance were averaged, evident outliers removed. If two inconsistent values or groups of values were reported, they were presented together with a note. All temperatures are in kelvin rounded to whole numbers. The data for single crystal X-ray studies (Tables 5 and 6) were taken from the CSD and analysed using standard software. Original structural studies are denoted in the tables by CSD reference codes (refcodes) that allow one to extract a full reference from the CSD.

Mass and charge distribution moments were calculated for disubstituted molecules using optimised geometry. Components of the diagonalised tensor of inertia

$$I_{ii} = \sum m_i r_{ij}^2, \qquad (6)$$

(where m_i are atomic masses, r_{ij} is a distance of j-th atom by i-th coordinate from centre of mass, $j = x, y, z$) were calculated directly. Components of dipole moment

$$\mu_i = \int \rho(\boldsymbol{r}) r_i \mathrm{d}\boldsymbol{r}, \qquad (7)$$

and components of a diagonalised traceless quadrupole moment[6]

$$Q_{ii} = (1/2) \int \rho(\boldsymbol{r})[3r_i r_j - r^2\delta_{ij}]\mathrm{d}\boldsymbol{r} \qquad (8)$$

(where $\rho(\boldsymbol{r})$ is electron density, r_i is projection of $\boldsymbol{r}$ on coordinate $i = x,y,z$, δ_{ij} is Kroneker delta and integration is done in a volume V) were calculated *ab initio* (HF 3-21G) by the GAUSSIAN 98 programme (Tables 9 and 10).

Results and discussion

Background of the model

A strongly anisotropic short-range term in a crystal van der Waals field is essential to reproduce theoretically the observed regularities of mp among crystals composed of medium-size molecules. A short-range *repulsion* term that correctly reflects the topology of a molecular field is widely used in theories of molecular condensed state,[6,8] in particular liquid crystals

Table 8 Total area (S_0) and asymmetry of section (a_s), and normalised group order (Δ) of Br-substituted benzenes in different van der Waals groups (data for sets of isomers under highest G are in bold)

Positions of Br		1	1,2	1,3	1,4	1,2,3	1,2,4	1,3,5	1,2,3,4	1,2,3,5	1,2,4,5
S_0, Å^2		40.78	45.82	46.68	46.69	51.86	51.65	52.55	56.69	57.71	56.58
a_s	C_s	0.002	0.004	0.0	0.006	0.0	0.057	0.004	0.004	0.0	0.0
	C_2	0.073	0.057	0.097	0.0	0.063	0.064	0.149	0.059	0.088	0.0
	C_{2v}	0.074	**0.059**	**0.097**	**0.006**	0.063	0.095	0.151	**0.061**	**0.088**	**0.0**
	C_3	0.110	0.093	0.112	0.157	0.081	0.141	0.001	0.102	0.081	0.141
	C_{3v}	0.111	0.095	0.112	0.159	**0.081**	**0.153**	**0.005**	0.104	0.081	0.141
	C_4	0.132	0.106	0.159	0.131	0.090	0.156	0.180	0.114	0.135	0.140
	C_{4v}	0.133	0.107	0.159	0.134	0.090	0.165	0.181	0.114	0.135	0.140
	C_6	0.135	0.110	0.165	0.157	0.106	0.162	0.149	0.120	0.133	0.141
	C_{6v}	0.136	0.112	0.165	0.160	0.106	0.175	0.152	0.121	0.133	0.141
Δ	C_s	1.92	1.84	2.00	1.79	2.00	0.64	1.83	1.84	2.00	2.00
	C_2	0.46	0.64	0.29	2.00	0.57	0.55	0.10	0.62	0.34	2.00
	C_{2v}	0.91	**1.22**	**0.58**	**3.58**	1.14	0.59	0.20	**1.19**	**0.69**	**3.99**
	C_3	0.33	0.47	0.32	0.13	0.60	0.18	2.97	0.39	0.59	0.18
	C_{3v}	0.66	0.91	0.64	0.25	**1.19**	**0.28**	**5.46**	0.76	1.18	0.36
	C_4	0.28	0.48	0.17	0.29	0.67	0.18	0.11	0.41	0.27	0.25
	C_{4v}	0.56	0.93	0.33	0.55	1.33	0.30	0.21	0.81	0.54	0.49
	C_6	0.40	0.67	0.22	0.26	0.72	0.24	0.31	0.55	0.42	0.36
	C_{6v}	0.79	1.29	0.44	0.49	1.44	0.36	0.58	1.06	0.84	0.71

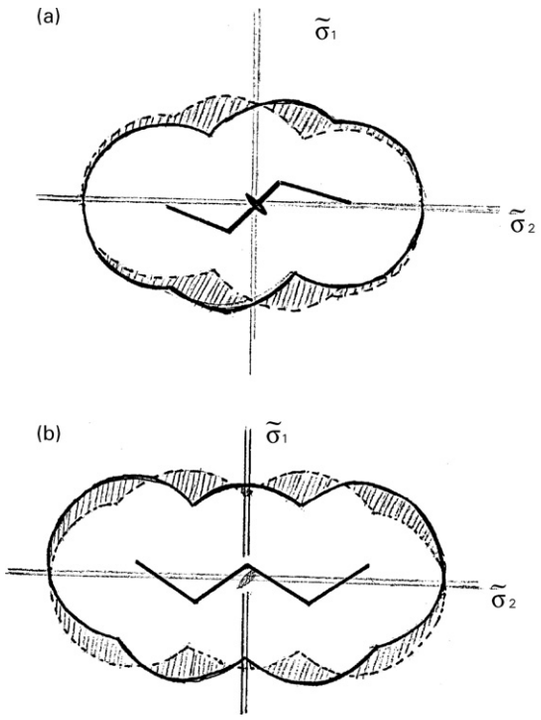

Fig. 4 Sections of van der Waals surfaces of *n*-butane (a) and *n*-pentane (b) molecules; CH_3 and CH_2 fragments represented by circles of the same radii. Strict symmetry elements are shown in black, approximate elements of C_{2v} group in grey. Misfit areas for $\tilde{\sigma}_2$ approximate mirror plane are shaded.

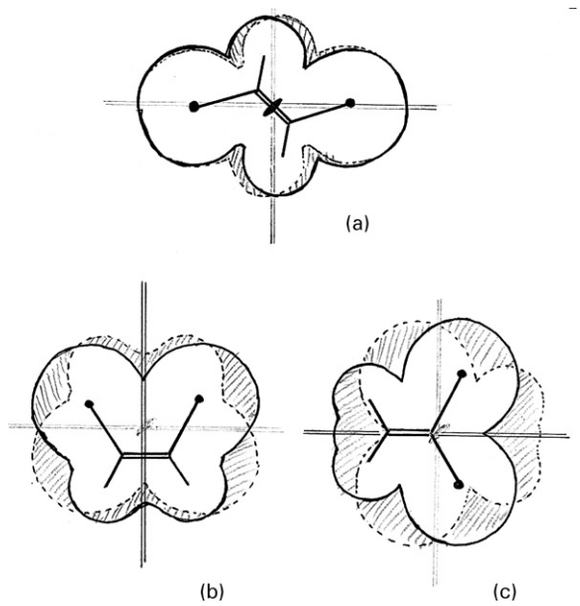

Fig. 6 Sections of molecular van der Waals surface for dichloroethylene isomers (solid line), their transformations by σ mirror planes (dotted line) and misfit areas (shaded): (a) *trans*-ClCH=CHCl, $a_s = 0.028$, mp 223 K (b) *cis*-CHCl=CHCl, $a_s = 0.072$, mp 192 K, (c) *gem*-CH_2=CCl_2, $a_s = 0.109$, mp 151 K. Exact symmetry elements are shown in black, approximate elements of C_{2v} group in grey.

(LC),[22–25] based on hard-core molecular models. (The attractive term that pulls molecules together is replaced in such models by artificial external limits, *e.g.* walls of a box).

Importance of molecular shape (*e.g.* of space-filling models) is widely acknowledged on a qualitative level in chemistry. Many theoretical schemes that utilize molecular shape factorisation were applied in studies of condensed phases (see *e.g.* refs 26–30). Particularly close to our approach is the surface tensor model suggested by Ferrarini *et al.*[28,29] where molecular potential in a liquid crystal was expanded into modified spherical harmonics and integrated over a molecular surface composed of atomic van der Waals spheres. This model, later confined by its authors to simplified molecular shapes like disks and rods, allowed them to reproduce a number of structure-dependent properties of LC phases.[25] Similar to the cited works, a concept of molecular van der Waals symmetry is easy to extend to a set of conformers with relative energies $\{E_i\}$ considering a weighted sum of molecular surfaces with $\exp(-E_i/kT)$ as weights (where k is the Boltzmann constant and T is temperature). Analysis of van der Waals molecular symmetry is therefore consistent with the results obtained earlier in physics and chemistry of molecular crystals but allows a theoretical interpretation of much more complex systems than before.

Even and odd *n*-alkanes

Sections of van der Waals surfaces for *n*-butane and *n*-pentane with their approximate symmetry elements in the D_{2h} group and (shaded) misfit areas are shown in Fig. 4 (where CH_2 and CH_3 units are shown by circles of the same diameter for simplicity). Note that all-*trans* carbon chains with an even and odd number of carbon atoms have different exact point groups C_{2h} and C_{2v}, respectively. Due to the existence of a horizontal σ_h mirror plane, we will discuss only corresponding "partial" G' groups of planar sections, in this case C_2 ("even"

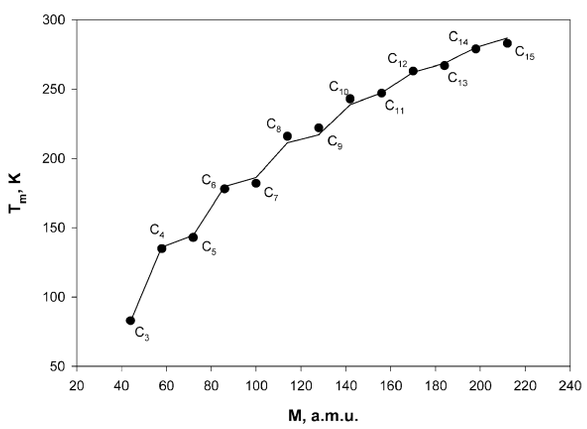

Fig. 5 Melting points of *n*-alkanes C_nH_{2n+2} (n = 3–15) *vs.* molecular mass (a.m.u.). Solid line: values calculated from a linear regression $T_m^{calc} = 119.7\ \ln M - 2416.5\ a_s - 216.3$ taking into account van der Waals asymmetries a_s (Table 7). Black dots: experimental data.

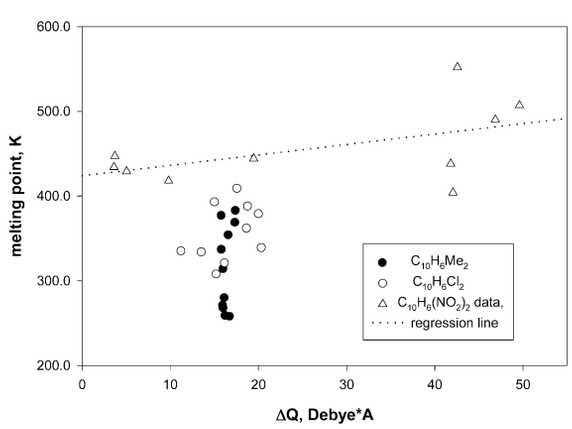

Fig. 7 Melting points *vs.* calculated ΔQ (GAUSSIAN 98, HF 3-21G) for isomers of disubstituted naphthalenes $C_{10}H_6X_2$: X = Me (filled circles), X = Cl (open circles) and X = NO_2 (open triangles). A tentative regression line in $C_{10}H_6(NO_2)_2$ set is shown by dots).

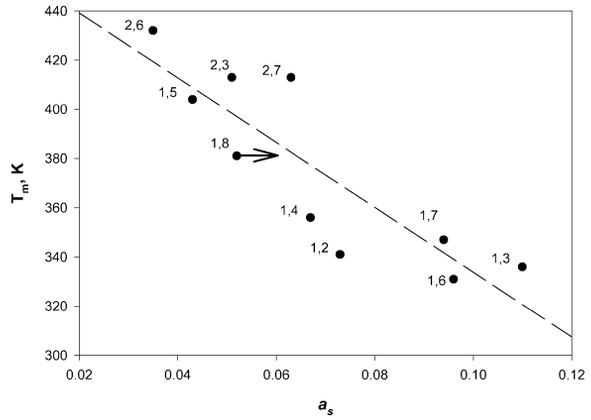

Fig. 8 Melting points *vs.* van der Waals asymmetry a_s for isomers of dibromonaphthalene $C_{10}H_6Br_2$. Additional shift of a_s for non-planar 1,8-isomer, not defined by the model of planar molecular section, is shown by an arrow. Dashes: a regression line.

chains), C_s (''odd'' chains) and C_{2v} (van der Waals group, see the previous chapter).

Positions of the approximate symmetry elements of the C_{2v} group relative to the molecule are dictated by the chain's exact symmetry. In ''odd'' *n*-alkanes, the longitudinal approximate mirror plane $\tilde{\sigma}_2$ goes along the chain normal to the exact mirror plane $\tilde{\sigma}_1$ creating an approximate twofold axis C_2 at their intersection. Contrary, in ''even'' chains two mutually perpendicular approximate $\tilde{\sigma}_1$ and $\tilde{\sigma}_2$ planes intersect along the actual C_2 axis. Subsequently, a longitudinal $\tilde{\sigma}_2$ plane in even *n*-alkanes passes along the chain diagonally from one terminal CH_3 group to the other, minimising a misfit area between the original and reflected sections better than in odd *n*-alkanes. In a very long ''odd'' chain, all atoms are displaced by a longitudinal $\tilde{\sigma}_2$ plane roughly by the same distance $L = (d/2)\sin(90^\circ - \theta/2) \approx 0.44$ Å (where $d = 1.54$ Å is C–C bond length, $\theta = 109.5^\circ$ is CCC bond angle), but in a long ''even'' chain the shift of atomic positions gradually decreases from L for a pair of central atoms to almost 0 for terminal groups. As a result, the asymmetry of ''odd'' chains towards the $\tilde{\sigma}_2$ plane is larger than ''even'' ones. As can be seen in Fig. 4, any of two approximate symmetry elements, related by an exact symmetry operation, has the same misfit area in its molecule, so the group asymmetry $a_s(C_{2v})$ simply equals $a_s(\sigma_v)/2$ both in ''even'' and ''odd'' chains.

As a result, the van der Waals surface of all-*trans* ''even'' chain is *more symmetric* than an ''odd'' chain of a comparable length, which means smaller deviation of the ''even'' chain from a higher van der Waals point group (C_{2v} for section or D_{2h} for 3D molecular surface). Considering asymmetry as a perturbation of the molecular field in the crystal, we may

Table 9 Moments of inertia I_{ii} ($\times 10^{-37}$ g cm^2), dipole moments μ (debye, D), quadrupole moments Q_{ii} (D Å) and $\Delta Q = \max(Q_{ii} - Q_{jj})$ ($i,j = x,y,z$) in mono- and disubstituted benzenes calculated with PM 3 optimised geometry. Electric moments were calculated *ab initio* (3-21G). *Italic*: data calculated by Syvitsky and Burnell in local density approximation (6-311++G**)[36]

Compound	I_{xx}	I_{yy}	I_{zz}	$\sum I_{ii}$	$\lvert\mu\rvert$	Q_{xx}	Q_{yy}	Q_{zz}	ΔQ
C_6H_5Me	0.15	0.33	0.47	0.95	0.33	3.11	3.24	−6.34	9.58
					0.45	*4.39*	*3.37*	*−7.77*	*12.16*
C_6H_5F	0.15	0.33	0.48	0.95	1.96	−1.25	5.99	−4.74	10.73
C_6H_5Cl	0.15	0.52	0.67	1.34	2.19	−0.67	5.99	−5.32	11.31
					1.67	*1.33*	*6.35*	*−7.67*	*14.02*
C_6H_5Br	0.15	0.82	0.97	1.94	1.83	0.55	5.37	−5.92	11.29
$C_6H_5NO_2$	0.21	0.68	0.88	1.76	5.54	−3.37	5.14	−1.77	8.51
C_6H_5OH	0.15	0.32	0.47	0.93	1.65	5.09	1.31	−6.40	11.49
o-$C_6H_4Me_2$	0.27	0.38	0.64	1.29	0.56	2.95	3.18	−6.14	9.32
					0.71	*3.70*	*3.35*	*−7.05*	*10.72*
m-$C_6H_4Me_2$	0.23	0.47	0.69	1.39	0.32	3.54	2.77	−6.30	9.84
					0.48	*4.55*	*3.08*	*−7.64*	*12.19*
p- $C_6H_4Me_2$	0.16	0.57	0.72	1.44	0.00	2.81	3.54	−6.35	9.89
					0.00	*2.37*	*5.47*	*−7.85*	*13.33*
o-$C_6H_4F_2$	0.26	0.38	0.64	1.28	3.37	0.98	2.29	−3.27	5.56
m-$C_6H_4F_2$	0.23	0.48	0.71	1.42	1.94	−4.19	6.48	−2.29	10.67
p-$C_6H_4F_2$	0.15	0.59	0.74	1.48	0.00	−1.75	9.93	−8.18	18.11
o-$C_6H_4Cl_2$	0.24	0.51	0.75	1.49	3.32	1.41	3.53	−4.94	8.47
					2.34	*2.71*	*5.01*	*−7.72*	*12.73*
m-$C_6H_4Cl_2$	0.29	0.96	1.25	2.51	2.08	−3.45	6.93	−3.48	10.41
					1.56	*−3.41*	*8.93*	*−5.52*	*14.45*
p-$C_6H_4Cl_2$	0.15	1.23	1.38	2.76	0.00	−7.23	10.00	−2.77	17.23
					0.00	*−6.90*	*11.04*	*−4.13*	*17.93*
o-$C_6H_4Br_2$	0.24	0.69	0.94	1.88	2.52	3.73	2.43	−6.17	9.90
m-$C_6H_4Br_2$	0.37	2.20	2.57	5.15	1.69	−1.47	6.31	−4.85	11.16
p-$C_6H_4Br_2$	0.15	2.86	3.01	6.02	0.00	−4.21	8.52	−4.32	12.84
o-C_6H_4MeCl	0.29	0.54	0.82	1.65	1.89	5.33	0.09	−5.42	10.75
					1.46	*4.04*	*3.22*	*−7.26*	*11.30*
m-C_6H_4MeCl	0.25	0.69	0.94	1.88	2.40	−0.12	4.97	−4.85	9.82
					1.99	*2.44*	*4.63*	*−7.07*	*11.70*
p-C_6H_4MeCl	0.15	0.85	1.00	2.00	2.61	6.46	−1.94	−4.52	10.98
					2.15	*5.79*	*1.34*	*−7.13*	*12.92*
o-$C_6H_4(NO_2)_2$	0.73	0.74	1.47	2.94	7.88	4.14	−6.53	2.38	10.67
m-$C_6H_4(NO_2)_2$	0.43	1.43	1.86	3.72	5.19	−18.87	10.99	7.88	29.86
p-$C_6H_4(NO_2)_2$	0.27	1.81	2.08	4.16	0.00	10.77	14.89	−25.66	40.55
o-$C_6H_4(OH)_2$	0.26	0.37	0.63	1.25	2.83	−0.45	6.86	−6.41	13.27
m-$C_6H_4(OH)_2$	0.22	0.46	0.68	1.36	1.63	0.83	5.38	−6.21	11.59
p-$C_6H_4(OH)_2$	0.15	0.56	0.71	1.42	0.00	7.24	−1.36	−5.88	13.12

Table 10 Molecular masses M (a.m.u.), experimental (μ_{exp}) and calculated molecular electric moments at HF 3-21G[a] and B3LYP 6-31G[b] levels for fluorinated ethylenes

Compound	M/a.m.u.	μ_{exp}/D	$\mu_{3\text{-}21G}$/D	$\Delta Q_{3\text{-}21}$/D Å	$\mu_{6\text{-}31G}$/D	$\Delta Q_{6\text{-}31G}$/D Å	T_m/K	T_b/K
C_2H_4	28	0	0	3.77	0	3.15	104	169
CH_2CHF	46	1.40	1.77	3.77	1.21	3.24	112	201
CH_2CF_2	64	1.40	1.91	2.51	1.19	2.05	[c]	189
CHFCHF								
cis-	64	2.40	3.08	2.93	2.12	2.53	172	247
trans-	64	0	0	8.62	0	5.74	185	221
$CHFCF_2$	82	[c]	1.87	5.30	1.25	3.57	[c]	221
C_2F_2	100	0	0	5.47	0	2.77	130	197

[a] Geometry optimised at PM 3 level. [b] With full geometry optimisation. [c] Not available.

conclude that *n*-alkanes C_nH_{2n+2} (and all other compounds with planar zigzag chain molecules) with an even 'n' would have elevated melting points in comparison with their "odd" homologues, which is the case. Predicted mp alterations between "even" and "odd" chains should converge when positional shifts $\Delta L_{i,i+2}$ between two neighbouring units on the same side of a chain approach *ca.* 0.1 Å, which is the approximate error in crystallographic van der Waals radii.[5] Since, for geometric reasons, $\Delta L_{i,i+2} = 4L/(n-1)$, one may estimate the upper limit of mp alternation as $n \leq 20$ in a good agreement with experimental data.

Average asymmetries $a_s(C_{2v})$ for C_nH_{2n+2} molecules with $n = 3$–15 in the C_{2v} group, calculated taking into account van der Waals radii of C and H atoms, are presented in Table 7 together with their molecular masses M and melting points T_m. The experimental T_m^{exp} values were fitted to the empirical regression line

$$T_m = 119.7 \ln M - 2416.5a_s - 216.3 \qquad (9)$$

that gives calculated T_m^{calc} values in Table 7. Calculated and observed data (Fig. 5) are in a reasonably good agreement, taking into account the simplicity of the applied model. Alterations of several other bulk properties (*e.g.* temperature and entropy of transition into isotropic liquid) were reported for LC whose molecules contain two rigid moieties with even- or odd-unit chains between them.[24,25]

Disubstituted ethylenes and substituted benzenes

Sections of van der Waals surfaces for disubstituted ethylenes $C_2H_2Cl_2$, their misfit areas, and asymmetries are shown in Fig. 6. Variations of molecular asymmetry between isomers, as well as "almost C_{2v}" symmetry of molecular section for *trans*–ClCH=CHCl (*i.e.* closeness of its 3D molecular shape to D_{2h} symmetry), are clearly visible. The increase of calculated a_s from *trans*- (0.028) to *cis*- (0.072) and *gem*-isomers (0.109) may be compared to a decrease of mp in the same sequence (223 K, 192 K and 151 K, respectively). Notwithstanding strong differences in van der Waals asymmetry, all isomers have exact point groups of the same order of 4. Moreover, *cis*- and *gem*-isomers have the same C_{2v} point symmetry (see Scheme 3)—so van der Waals shape of a molecule gives more information than its atomic structure.

Similar a_s order is observed in other disubstituted ethylenes (*e.g.* $C_2H_2Br_2$ isomers: *trans*- 0.042, *cis*- 0.171 *gem*- 0.273; mp's are not available in this set). Note, however, that rather large deviations of *cis*- and especially *gem*-isomers with bulky substituents from C_{2v} symmetry of a molecular section can hardly be considered as small perturbations, which is a basic assumption in our model. Strong dissimilarity in molecular shape may alter packing pattern destroying correlations (*cf.* mp order *gem*- ≈ *cis*- < *trans*- for dimethylethylenes in Table 1).

Molecular van der Waals sections of disubstituted benzene isomers deviate from C_{2v} symmetry in "*p*- < *o*- < *m*-" order (Table 8), which resembles *trans*- < *cis*- < *gem*- sequence in the $C_2H_2X_2$ family. Melting points of the isomers decrease in the same row. As in disubstituted ethylenes, van der Waals asymmetries allow one to distinguish between "more symmetric" *ortho*- and "less symmetric" *meta*-isomers regardless of their same exact point group. Note that, unlike *trans*-XCH=CHX, a section of *para*-$C_6H_4X_2$ for X = halogen (but not Me) has exact C_{2v} symmetry.

In Table 8, average asymmetries $a_s(\check{G})$ and normalised group orders Δ in nine different van der Waals groups [formula (5) with empirical weight $\gamma = 20$] for mono- to tetrasubstituted benzenes $C_6H_{6-n}X_n$ (X = Br) are presented. The asymmetry for these "rounded" molecules does not exceed 0.20, increasing with the increase of the group order, and yet differs significantly among the isomers in each group. The normalised group order Δ, defined rather empirically at the moment, allows us to select the closest point group for each isomer and reveals the same trend as molecular asymmetries in each set of isomers. In particular, relative values of both a_s (in decreasing order) and Δ (in increasing order) parallel the correct experimental mp trend, *viz.* *m*- < *o*- < *p*- in disubstituted, 1,2,4- < 1,2,3- < 1,3,5- in trisubstituted and 1,2,3,5- < 1,2,3,4- < 1,2,4,5- in tetrasubstituted benzenes. This result, determined by a geometry of nuclear positions, is quite robust and completely reproducible for other X substituents (Me, Cl).

Melting points *vs.* moments of mass and charge distributions

An alternative viewpoint that exists in the literature links the observed mp trends in organic compounds as well as their other bulk properties, to differences in moments of the mass and charge distributions in corresponding molecules.[31] An influence of dipole–quadrupole (***μ*–*Q***) and quadrupole–quadrupole (***Q*–*Q***) interactions on molecular packing of aromatic compounds was discussed extensively during the last decade.[32–35] To check this possible alternative, we calculated the electric dipole [formula (7)] and traceless electric quadrupole [formula (8)] charge distribution moments, as well as the inertia moments, for disubstituted benzenes and naphthalenes at HF 3-21G and PM 3 levels of theory, respectively (see Calculations). The results are presented in Table 9.

Calculated components of dipole and quadrupole moments generally agree both with the results of calculations obtained by Syvitsky and Burnell on a more sophisticated level of theory[36] and with the experimental data.[3,6,37] It should be noted that measured dipole moments for medium-size molecules in the Beilstein database[3] may vary by factor of 2, whereas experimental quadrupole moment values[6,38,39] are rather scarce and may differ by an order of magnitude, as well as by sign, between data for the same substance obtained by different authors and, especially, using different methods. The inertia moment, completely determined by optimised geometry, has been calculated with high precision.

Data in Table 9 show a lack of notable correlation between calculated moments and melting points. In most cases, I_{ii} and ΔQ, where $\Delta Q = \max(Q_{ii} - Q_{jj})$ for a same molecule, increase in *o-* < *m-* < *p-* sequences. Calculated dipole moments $|\mu|$, in agreement with experimental data, decrease in the *o-* > *m-* > *p-* order, vanishing for centrosymmetric *para*-$C_6H_4X_2$ molecules. Deviations of our calculated ΔQ from the *o-* < *m-* < *p-* sequence are observed for chlorotoluenes whose *meta*-isomer melts lower (225 K) than the *ortho*-isomer (237 K), as well as for catechol (*o*-) and resorcinol (*m*-) isomers of $C_6H_4(OH)_2$ where the *meta*-isomer actually melts higher than the *ortho*-isomer by 6 K (see Table 5). However, more accurate LDF calculations with a 6-311++G** basis set have given a general *o-* < *m-* < *p-* order of ΔQ for chlorotoluenes,[36] so the calculated ΔQ values do not correspond to a true mp sequence. Electric moments of fluoro-substituted ethylenes, calculated by us at two levels of theory (HF 3-21G and B3LYP with 6-31G basis set), show a *cis-* > *gem-* > *trans-* order for the dipole (zero for *trans*-FCH=CHF) and *gem-* ≤ *cis-* < *trans-* for the quadrupole moment (Table 10). Although the order of ΔQ in disubstituted ethylenes is closer to the observed mp data (which is not available for *gem*-difluoroethylene), electric moments in a total C_2H_4–C_2F_4 series, shown in Table 10, display no definite correlations with mp or b.p. data. (Note also the decreased melting and boiling points of polyfluorinated species $CHF{=}CF_2$ and $CF_2{=}CF_2$ despite their larger molecular masses, which reflects an influence of destabilising F···F repulsion in a condensed phase.[15]) We may conclude that the observed trends in mp among isomers of disubstituted benzenes and ethylenes are not determined solely by their mass and electric moments that may only modify the molecular field to some extent.

The irrelevance of electric moments to mp trends in substituted benzenes is qualitatively illustrated by the high mp of 1,3,5-$C_6H_3X_3$ derivatives with electron–acceptor X substituents (*e.g.* F), where $\mu = 0$ and $\boldsymbol{Q}$ is small on electrostatic grounds. The existence of the same mp trend among isomers with polar (halogen, NO_2) and non-polar (Me) substituents gives another strong argument against electrostatic origins of the observed effect. However, a large quadrupole electric moment can have a notable effect on the mp which is apparent from a comparison of dicyano- $C_6H_4(CN)_2$ and di-isocyanobenzenes $C_6H_4(NC)_2$ (see Table 4). Despite a very similar linear geometry of C_{Ph}–CN (d_{CC} = 1.443 Å, d_{CN} = 1.138 Å) and C_{Ph}–NC fragments (1.399 Å and 1.144 Å, respectively, CSD[40]), all dicyano-isomers where the quadrupole moment is larger, due to larger distances of the electronegative N atoms from the centre of benzene ring, melt at *ca.* 60 K higher then their isocyano analogues. Note also that both sets of isomers deviate from the "*m-* < *o-* < *p*" mp trend.

The most prominent influence of electrostatic forces on the mp may be seen in polyfluorinated organic compounds whose mp and b.p. are strongly reduced due to destabilising $F^{\delta-}\cdots F^{\delta-}$ intermolecular repulsion[15,16] as well as in compounds with intermolecular H-bonding that has a large electrostatic component.[8,41] Both factors shift the mp (in opposite directions) within sets of isomers and may alter mp trends in some of them, as discussed above. In less-polarised molecules, electrostatic intermolecular terms exert a minor influence on the mp in comparison with van der Waals forces, as can be seen from a good correlation of "*m-* < *o-* < *p-*" trend in disubstituted benzenes with their molecular asymmetries a_s and a lack of correlation with the molecular electric moments.

Disubstituted naphthalenes

Calculated asymmetries of van der Waals sections in the C_{2v} group for ten isomers of dibromonaphthalenes $C_{10}H_6Br_2$ (see Table 6) qualitatively reproduce the observed mp trend, revealing four more symmetric isomers with lower $a_s = 0.035 - 0.063$ (1,5-, 2,3-, 2,6- and 2,7) and three less symmetric ones with higher $a_s = 0.094 - 0.110$ (1,3-, 1,6- and 1,7-) with 1,2- (0.073), 1,4- (0.067) and 1,8-isomers $(0.052 + x)$ in between. Note that the 1,8-isomer with a non-planar naphthalene core, due to steric repulsion of the substituents (CSD), is not consistent with our model of planar molecular sections. Therefore, it should have some additional asymmetry value '*x*', caused by a break in the σ_h mirror plane.

Calculated moments of charge distribution for disubstituted naphthalenes show a poor correlation with their mp (Fig. 7). For dinitronaphthalenes where electric moments are highest, only a very loose tendency for a slow increase of T_m with the increase of ΔQ may be noticed (white triangles in Fig. 7). However, a similar trend in melting points between geometric isomers of dimethylnaphthalenes, whose electric quadrupole moments lie in very narrow limits (black dots in the same Fig. 7) attests to the minor role of electrostatic forces as compared to van der Waals forces, in the observed mp regularities. At the same time, van der Waals section asymmetries, display much better correlation with melting points (Fig. 8, where an additional '*x*' value for 1,8-isomer is denoted by an arrow). The relative impact of van der Waals and electrostatic forces on the mp of naphthalenes and larger molecules bearing strong acceptor substituents, will be studied in more detail.

Conclusions and prospects

Based on our present results, we may suggest that the analysis of molecular van der Waals symmetry opens a promising new way for a theoretical interpretation of the observed trends in melting point and probably other properties that are strongly related to intermolecular interactions. It affords a physically consistent interpretation for long-known effects like "even–odd" mp alteration in alkanes or "*meta-* < *ortho-* < *para*" mp sequence in disubstituted benzenes. At the same time, van der Waals symmetry provides a more distinct border between true van der Waals crystals and the compounds whose bulk properties are influenced by other factors like electrostatic and specific interactions. The proposed formalism therefore deserves further development.

Three most obvious directions where van der Waals symmetry might be successfully applied are (i) analysis of mp trends in other organic and organometallic compounds, (ii) consideration of other bulk properties of condensed phases influenced by intermolecular interactions, and (iii) extension to other types of symmetry—first of all, analysis of van der Waals space groups of molecular packing. Studies in the first direction may help to understand a proper choice of van der Waals group in various sets of substances as well as a role of strong electrostatic effects therein (*e.g.* in disubstituted carboranes $C_2B_{10}H_{10}X_2$ where a "*p-* < *m-* < *o-*" sequence of mp is observed relative to positions of X substituents). In the second direction, our current analysis of b.p. trends[15] may further be extended to the properties of liquid crystals and to solubility. The third direction looks particularly promising since van der Waals symmetry of crystal packing patterns might help to rationalise such long-known phenomena in molecular crystals as preferred and forbidden space groups,[5] isomorphism, polymorphism, existence of symmetrically independent molecules,[42] and pseudosymmetry.[43]

Acknowledgements

Financial support from the Royal Society of London is gratefully acknowledged by Y.L.S. The work was also partially supported by a grant 02-03-33225 from the Russian Foundation for Basic Research. The authors are indebted to Charlotte Broder for CSD data on *m-* and *p*-isomers of disubstituted

benzenes and to Dr Dmitry Yufit for data on single crystals study of *o*- and *p*-diethylbenzene grown from a liquid,[17] useful references and stimulating discussion. J.A.K.H. thanks the EPSRC for a Senior Research Fellowship.

References

1 F. H. Allen, S. Bellard, M. C. Brice, B. A. Cartwright, A. Doubleday, H. Higgs, T. Hummelink, B. G. Hummelink-Peters, O. Kennard, W. D. S. Motherwell, J. R. Rodgers and D. G. Watson, *Acta Crystallogr., Sect. B*, 1979, **35**, 2331.
2 G. Bergerhoff, R. Hundt, R. Sievers and I. D. Brown, *J. Chem. Inf. Comput. Sci.*, 1983, **23**, 66.
3 Beilstein Institut zur Förderung der Chemischen Wissenschaften licenced to Beilstein Chemie Daten und Software GmbH and MDL Information Systems GmbH, Version 4, December 2002.
4 2002 Gesellschaft Deutscher Chemiker licensed to MDL Information Systems GmbH, Version 4, December 2002.
5 A. Kitaigorodskii, *Molecular Crystals and Molecules*, Academic Press, New York, 1973.
6 C. E. Gray and K. E. Gibbins, *Theory of Molecular Fluids*, Clarendon, Oxford, 1984, vol. 1.
7 G. R. Desiraju, *Crystal Engineering: the Design of Organic Solids*, Elsevier, Amsterdam, 1989.
8 J. Israelachvili, *Intermolecular & Surface Forces*, 2nd edn., Academic Press, New York, 1991.
9 *Structure Correlation*, eds. H.-B. Bürgi and J. D. Dunitz, WCH, Weinheim, 1994.
10 C. Tsallis, *Chaos Solitons Fractals*, 2002, **13**, 371.
11 H. F. Herbrandson and F. C. Nachod, in *Determination of Organic Structures by Physical Methods*, eds. E. S. Braude and F. C. Nachod, Academic Press, New York, 1955, p. 3.
12 R. Boese, H. C. Weiss and D. Blaser, *Angew. Chem., Int. Ed.*, 1999, **38**, 988.
13 A. D. Bond, BCA Spring Meeting 2003, Abstracts, CP-40, p. 63.
14 R. Boese, M. T. Kirchner, J. D. Dunitz, G. Filippini and A. Gavezotti, *Helv. Chim. Acta*, 2001, **84**, 1561.
15 Yu. L. Slovokhotov and J. A. K. Howard, 2003, in preparation.
16 V. R. Thalladi, H.-C. Weiss, D. Bläser, R. Boese, A. Nangia and G. R. Desiraju, *J. Am. Chem. Soc.*, 1998, **120**, 8702.
17 D. S. Yufit, Yu. L. Slovokhotov, I. S. Neretin and J. A. K. Howard, 2003, in preparation.
18 A. Gavezotti, in *Structure Correlation*, eds. H.-B. Bürgi and J. D. Dunitz, WCH, Weinheim, 1994 vol. 2, p. 509.
19 A. Bondi, *J. Phys. Chem.*, 1964, **68**, 441.
20 F. A. Cotton, *Chemical Applications of Group Theory*, 3rd edn., Wiley, New York, 1990.
21 Gaussian 98, Revision A.3, M. J. Frisch, G. W. Trucks, H. B. Schlegel, G. E. Scuseria, M. A. Robb, J. R. Cheeseman, V. G. Zakrzewski, J. A. Montgomery, Jr., R. E. Stratmann, J. C. Burant, S. Dapprich, J. M. Millam, A. D. Daniels, K. N. Kudin, M. C. Strain, O. Farkas, J. Tomasi, V. Barone, M. Cossi, R. Cammi, B. Mennucci, C. Pomelli, C. Adamo, S. Clifford, J. Ochterski, G. A. Petersson, P. Y. Ayala, Q. Cui, K. Morokuma, D. K. Malick, A. D. Rabuck, K. Raghavachari, J. B. Faresman, J. Cioslowski, J. V. Ortiz, B. B. Stefanov, G. Liu, A. Liashenko, P. Piskorz, I. Komaromi, R. Gomperts, R. L. Martin, D. J. Fox, T. Keith, M. A. Al-Laham, C. Y. Peng, A. Nanayakkara, C. Gonzalez, M. Challacombe, P. M. W. Gill, B. Johnson, W. Chen, M. W. Wong, J. L. Andres, C. Gonzalez, M. Head-Gordon, E. S. Replogle and J. A. Pople, Gaussian Inc., Pittsburgh PA, 1998.
22 *Handbook of Liquid Crystals*, eds. D. Demus, J. Goodby, G. W. Gray, H.-W. Spiess and V. Vill, Wiley-VCH, Weinheim, 1998, vol. 1–3.
23 M. A. Osipov, in *Handbook of Liquid Crystals*, eds. D. Demus, J. Goodby, G. W. Gray, H.-W. Spiess and V. Vill, Wiley-VCH, Weinheim, 1998, vol. 1, p. 40.
24 D. Demus, in *Handbook of Liquid Crystals*, eds. D. Demus, J. Goodby, G. W. Gray, H.-W. Spiess and V. Vill, Wiley-VCH, Weinheim, 1998, vol.1, p. 133.
25 C. T. Imrie and G. R. Luckhurst, in *Handbook of Liquid Crystals*, eds. D. Demus, J. Goodby, G. W. Gray, H.-W. Spiess and V. Vill, Wiley-VCH, Weinheim, 1998, vol. 2B, p. 801.
26 D. Catalano, C. Forte, C. A. Veracini and C. Zannoni, *Isr. J. Chem.*, 1983, **23**, 283.
27 C. T. Yim and D. F. Gilson, *J. Phys. Chem.*, 1991, **95**, 980.
28 A. Ferrarini, G. J. Moro, P. L. Nordio and G. R. Luckhurst, *Mol. Phys.*, 1992, **77**, 1.
29 A. Ferrarini, G. R. Luckhurst, P. L. Nordsio and S. J. Roskilly, *J. Chem. Phys.*, 1994, **100**, 1460.
30 M. A. Spackman and J. McKinnon, *CrystEngComm*, 2002, **4**, 378.
31 B. D. Silvermann and D. E. Platt, *J. Med. Chem.*, 1996, **39**, 2129.
32 J. H. Williams, *Acc. Chem. Res.*, 1993, **26**, 593.
33 A. P. West, S. Mecozzi and D. A. Dougherty, *J. Phys. Org. Chem.*, 1997, **10**, 347.
34 F. Ponzini, R. Zagha, K. Hardcastle and J. S. Siegel, *Angew. Chem., Int. Ed.*, 2000, **39**, 2323.
35 J. A. C. Clyburne, T. Hamilton and H. A. Jenkins, *Cryst. Eng.*, 2001, **4**, 1.
36 R. T. Syvitsky and E. E. Burnell, *J. Chem. Phys.*, 2000, **113**, 3452.
37 A. L. McClellan, *Tables of Experimental Dipole Moments*, Freeman & Co, San Francisco, 1963.
38 W. H. Flygare and R. C. Benson, *Mol. Phys.*, 1971, **20**, 225.
39 M. A. Spackman, *Chem. Rev.*, 1992, **92**, 1769.
40 A. G. Orpen, L. Brammer, F. H. Allen, O. Kennard, D. G. Watson and R. Taylor, in *Structure Correlation*, eds. H.-B. Bürgi and J. D. Dunitz, WCH, Weinheim, 1994, vol. 2, p. 751.
41 J. Bernstein, M. C. Etter and L. Leiserovitz, in [9], vol. 2, p. 431.
42 J. W. Yao, J. C. Cole, E. Pidcock, J. A. K. Howard, F. Allen and W. D. S. Motherwell, *Acta Crystallogr., Sect. B*, 2002, **58**, 640.
43 P. M. Zorky, *J. Mol. Struct.*, 1996, **374**, 9.